

- Mechanism of vasculitis and aneurysms in Kawasaki disease: role of nitric oxide. *Nitric Oxide* **8**: 15-25, 2003.
- 12) Harada T, Miura NN, Adachi Y, Nakajima M, Yadomae T, Ohno N: IFN-gamma induction by SCG, 1,3-beta-D-glucan from *Sparassis crispa*, in DBA/2 mice *in vitro*. *J Interferon Cytokine Res* **22**: 1227-1239, 2002.
- 13) Nagi-Miura N, Harada T, Shinohara H, Kurihara K, Adachi Y, Ishida-Okawara A, Oharaseki T, Takahashi K, Naoe S, Suzuki K, Ohno N: Lethal and severe coronary arteritis in DBA/2 mice induced by fungal pathogen, CAWS, *Candida albicans* water-soluble fraction. *Atherosclerosis* **186**, 310-320, 2006.
- 14) Shinohara H, Nagi-Miura N, Ishibashi K, Adachi Y, Ishida-Okawara A, Oharaseki T, Takahashi K, Naoe S, Suzuki K, Ohno N: Beta-mannosyl linkages negatively regulate anaphylaxis and vasculitis in mice, induced by CAWS, fungal PAMPS composed of mannoprotein-beta-glucan complex secreted by *Candida albicans*. *Biol Pharm Bull* **29**, 1854-1861 2006.
- 15) Miura N, N, Miura T, Ohno N, Adachi Y, Watanabe M, Tamura H, Tanaka S, Yadomae T: Gradual solubilization of *Candida* cell wall beta-glucan by oxidative degradation in mice. *FEMS Immunol Med Microbiol* **21**, 123-129 1998.

Coronary Arteritis Induced by CAWS (*Candida albicans* Water-Soluble Fraction) in Various Strains of Mice

Noriko Nagi-Miura, Yoshiyuki Adachi, Naohito Ohno

Laboratory for Immunopharmacology of Microbial Products, School of Pharmacy, Tokyo University of Pharmacy and Life Science

The intraperitoneal administration of CAWS (water-soluble extracellular polysaccharide fraction obtained from the culture supernatant of *Candida albicans* NBRC 1385) to mice induces coronaritis similar to Kawasaki disease. We analyzed differences in the occurrence of coronary arteritis among mouse strains, inbred strains, a closed colony, hybrids and mutants. CAWS vasculitis was induced in almost all of the inbred and closed colony strains tested, except for CBA/J mice; it was induced also in hybrids, CDF1 and BDF1. In mutant strains of various immunological defects, such as C57BL/6J Ham *Slc-bg*, Balb/c *nu/nu*, C.B.17/*Icr-scid/scid*, WBB6F1-*W/W^s* mice, all induced CAWS vasculitis but a relatively weak phenotype. It has already been postulated that CAWS vasculitis is regulated by various genes, those related to acute as well as chronic inflammation. This might well reflect the clinical situation in human disease.

Highly Expressed Dectin-1 on Bone Marrow-Derived Dendritic Cells Regulates the Sensitivity to β -Glucan in DBA/2 Mice

Toshie Harada,¹ Noriko N. Miura,¹ Yoshiyuki Adachi,¹ Mitsuhiro Nakajima,²
Toshiro Yadomae,¹ and Naohito Ohno¹

Sparassis crispa β -glucan (SCG) is a major six-branched 1,3- β -D-glucan in *S. crispa* Fr. showing antitumor activity. We previously found that DBA/1 and DBA/2 mice are highly sensitive to SCG *in vivo* and *in vitro*. In this study, we investigated the effect of SCG on bone marrow-derived dendritic cells (BMDCs) in DBA/2 mice *in vitro*. SCG increased the expression of CD80, MHC class I and MHC class II molecules on the cell membrane of BMDCs. SCG induced BMDCs to produce interleukin-12p70 (IL-12p70), IL-6, and tumor necrosis factor- α (TNF- α). The magnitude of cytokine induction by SCG in DBA/2 mice was higher than that in C57BL/6, BALB/c, C3H/HeN, and C3H/HeJ mice. The expression level of the β -glucan receptor, dectin-1, on BMDCs in DBA/2 mice was also highest in DBA/2 among these mice. Blocking dectin-1 significantly inhibited the induction of TNF- α production by SCG. Taken together, these results suggest that the BMDCs from DBA/2 mice are highly sensitive to the induction of cytokine production by SCG *in vitro*, and that this sensitivity is related to the expression level of dectin-1.

Introduction

β -Glucans are important cell wall components of fungi. Some β -glucans are well-known biological response modifiers, and the mushrooms from which they are derived are widely distributed in nature and are used as medicine and food. Among the β -glucans, the six-branched 1,3- β -glucan is the best characterized. We have analyzed the mechanism of β -glucan-mediated immunopharmacological activity (Yadomae and Ohno 1996; Yadomae 2000). We and others have demonstrated that immunomodulating activity of β -glucans is mainly related to their effects on immune effector cells, such as macrophages, mononuclear cells, and neutrophils, involved in innate immunity, resulting in the production of cytokines (Yadomae and Ohno 1996; Yadomae 2000; Herre and others 2004). The body's defense against microbial attack and against spontaneously arising malignant tumor cells comprises a dynamic orchestrated interplay of innate and acquired immune responses, and the effectors of innate immunity can initiate these systems. The host defense system has receptors for β -glucans in order to recognize and

eliminate fungi, such as *Pneumocystis* and *Candida*, which generally contain β -glucan in their cell walls (Dennehy and Brown 2007). Orally administered β -1,3-glucan potentiated the activity of antitumor monoclonal antibody, leading to enhanced tumor regression and survival (Hong and others 2003). These findings indicated that β -glucan is an important player in both host defense against fungi and cancer immunotherapy.

Sparassis crispa is a medicinal mushroom. The primary component of the major ice-cold NaOH extracted polysaccharide fraction from *S. crispa* was found to be six-branched 1,3- β -glucan, having one branch approximately every third main chain (Ohno and others 2000; Tada and others 2007). This fraction showed strong antitumor activity against the solid form of Sarcoma 180 in ICR mice (Ohno and others 2000). In our previous study, we used *S. crispa* to treat several cancer patients in combination with lymphocyte transplantation immunotherapy and obtained a good response (Ohno and others 2003). To examine the pharmacological usefulness of *S. crispa* β -glucan (SCG), we purified SCG from the ice-cold

¹Laboratory for Immunopharmacology of Microbial Products, School of Pharmacy, Tokyo University of Pharmacy & Life Science, 1432-1 Horinouchi, Hachioji, Tokyo, Japan.

²Minahhealth Co., Kumagaya, Saitama, Japan.

NaOH extracted fraction. SCG enhanced the hematopoietic response in cyclophosphamide-induced leukopenic mice (Harada and others 2002a; Ohno and others 2002), and the effect was augmented by combination with isoflavone aglycone (Harada and others 2005). SCG stimulated leukocytes to produce cytokines in preparations of the human peripheral blood mononuclear cells (Nameda and others 2003), splenocytes from naïve DBA/1 and DBA/2 mice (Harada and others 2002b), and splenocytes from cyclophosphamide-treated mice (Harada and others 2002a; Harada and others 2006a). These results show that SCG can enhance immune responses *in vivo* and *in vitro*. The field of glucans has been confounded by the presence of endotoxin in glucan preparations. Endotoxin was not detected in SCG with determination by endoscopy (<30 pg/mg) (Harada and others 2006b). Therefore, SCG is also used as a purified soluble β -glucan in investigations on cellular receptors and molecular mechanisms (Sato and others 2006; Saijo and others 2007).

Powerful and well-orchestrated immune responses are essential for the host to eradicate infections and spontaneously arising malignant tumor cells. Dendritic cells (DCs) are professional antigen-presenting cells (APCs) that play a critical role in the induction of primary adaptive-immune responses (Banchereau and Steinman 1998). Because of this ability of DCs, strategies for targeting these cells *in vivo* have potential for use in various clinical settings (Sun and others 2006). Immature DCs distributed throughout peripheral tissues are specialized sentinels for antigen capture. Upon pathogen recognition, DCs are activated and migrate to secondary lymphoid organs, where they present pathogen-derived antigens to naïve T cells. Knowledge about the DC receptors involved in the recognition of pathogens, which include Toll-like receptors (TLRs) and C-type lectins, is starting to emerge (Thoma-Uszynski and others 2001; Figdor and others 2002). C-type lectins are characterized by a carbohydrate recognition domain (CRD), which interacts with pathogen-derived carbohydrate structures in a calcium-dependent manner (Drickamer 1999). The β -glucan receptor dectin-1 is a C-type lectin that we and others have previously demonstrated plays a crucial role in the detection of β -glucan and live pathogenic fungi by macrophages and DCs (Adachi and others 2004; Gantner and others 2005; Steele and others 2005; Saijo and others 2007). A recent report suggested that dectin-1 can directly activate nuclear factor- κ B (NF- κ B) in DCs via the signaling adaptor molecule CARD9 (Gross and others 2006). These reports indicated that dectin-1 is one of the key coordinators of macrophage/DC antimicrobial responses.

Previously, we reported that interferon- γ (IFN- γ) tumor necrosis factor- α (TNF- α) interleukin-12p70 (IL-12p70), and granulocyte-monocyte-colony stimulating factor (GM-CSF) production was not induced by SCG in splenocytes derived from inbred strains of mice, except for DBA/1 and DBA/2 mice (Harada and others 2002b; Harada and others 2004; Harada and others 2006c). DBA/1 and DBA/2 mice also produce significantly higher titers of antibody to SCG than other inbred naïve mice (Harada and others 2003). These results indicate that leukocytes derived from DBA/1 and DBA/2 mice are highly sensitive to SCG *in vivo* and *in vitro*. We also demonstrated that GM-CSF is a key molecule for cytokine

induction by β -glucan, and that GM-CSF is specifically induced by SCG in DBA/2 mice *in vitro* (Harada and others 2004; Harada and others 2006c). In this study, we investigated the effect of SCG on bone marrow-derived dendritic cells (BMDCs) in DBA/2 mice *in vitro*, and the relationship between reactivity to SCG and the expression of dectin-1 on BMDCs in DBA/2 mice.

Materials and Methods

Animals

C57BL/6, BALB/c, C3H/HeN, C3H/HeJ, and DBA/2 male mice between 6 and 7 weeks of age were purchased from Japan SLC (Shizuoka, Japan). The experimental protocol was approved by the Committee for Animal Care and Use (Tokyo University of Pharmacy and Life Science). Mice were maintained under specific pathogen free (SPF) conditions, at $23 \pm 1^\circ\text{C}$, with a constant humidity of $55 \pm 5\%$, under a cycle of 12 h of light and 12 h of dark, and had free access to food and tap water according to the Guidelines for Experimental Animal Care issued by the Prime Minister's Office of Japan.

Preparation of SCG

Fruit bodies of *S. crista* were cultured by Minahealth Co. (Saitama, Japan). SCG was prepared as described previously (Harada and others 2002a). In brief, air-dried and powdered *S. crista* was extracted with ice-cold alkali (10% NaOH/5% urea, 4°C , 2 days). The extract dissolved in 8 M urea was applied to a DEAE Sephadex A25 (Cl-) column equilibrated with 8 M urea, and the pass-through fraction was collected and extensively dialyzed against tap and distilled water, and then lyophilized (elemental analysis C:H:N = 40.06:6.77:0.08). SCG solution was prepared by dissolving the lyophilized powder in 0.5 N NaOH, followed by immediate dialysis against saline for 3 days. After dialysis, the dialyzed fraction was autoclaved and frozen until use.

Materials

Tween 20 was purchased from Wako Pure Chemical Co. (Osaka, Japan). Hank's balanced salt solution (HBSS) was purchased from Nissui Seiyaku Co., Ltd. (Tokyo, Japan). Gentamicin sulfate, RPMI 1640 medium, and bovine serum albumin (BSA) were from Sigma Chemical Co. (St. Louis, MO). Fetal calf serum (FCS) was from Sanko Junyaku Co., Ltd. (Tokyo, Japan). Recombinant mouse GM-CSF and recombinant mouse IL-4 were from BD Biosciences (USA).

Preparation of BMDCs

Bone marrow was removed from mice. Bone marrow cells obtained by flushing femoral shafts were suspended in HBSS containing 50 $\mu\text{g}/\text{ml}$ gentamicin sulfate. After centrifugation, the single cell suspension was treated with an ACK-lysing buffer (8.29 g/L NH₄Cl, 1 g/L KHCO₃, 37.2 mg/L EDTA/2Na) to lyse red blood cells. After centrifugation, the cells were maintained in RPMI 1640 medium supplemented with 50 $\mu\text{g}/\text{mL}$ gentamicin sulfate containing 5% heat-inactivated FCS, 10 ng/mL recombinant mouse GM-CSF, and

5 ng/mL recombinant mouse IL-4 and cultured in 24-well flat bottomed plates at 1×10^6 cells per well in 1 mL of culture medium at 37°C in a humidified 5% CO₂-95% air atmosphere. Nonadherent and loosely adherent cells were removed by pipetting on day 2 and replated with fresh cytokine-containing medium in the plate. SCG or lipopolysaccharide (LPS) was added on day 5. On day 7, nonadherent and loosely adherent cells or culture supernatant were collected.

Flow cytometry

BMDCs were stained with FITC- and PE-conjugated monoclonal antibodies (mAbs). To block the FcR-mediated binding of the mAb, antimouse CD16/CD32 FcBlockTM (BD Biosciences) was added. The cells were analyzed using a FACSCalibur, and the data were processed using the CELLQuest program. The following mAbs were used for immunofluorescent staining: FITC-antimouse dectin-1 (2A11; CellSciences, USA), FITC-antimouse CD11c (BD Biosciences), PE-antimouse CD80 (BD Biosciences), PE-antimouse H2Dd (BD Biosciences), PE-antimouse IAd (BD Biosciences), and PE-antimouse CD11c (BD Biosciences).

Measurement of cytokines

Concentrations of cytokines were measured using ELISA. All monoclonal antibodies and corresponding recombinant cytokines used were purchased from BD Biosciences.

Statistical analysis

The results are expressed as the means \pm standard deviation (SD). The significance of differences between the means was measured using Student's *t*-test.

Results

SCG induces maturation of BMDCs in DBA/2 mice

Immature DCs develop into mature DCs with the upregulation of MHC and costimulatory molecules in inflammatory microenvironments, and migrate to regional lymph nodes, where naive T cells are activated. The cell surface expression of MHC and costimulatory molecules is critical for the activation of naive T cells (Banchereau and Steinman 1998). To determine whether SCG could induce the maturation of BMDCs *in vitro*, we observed the phenotype of BMDCs treated with SCG. BMDCs from DBA/2 mice were cultured with SCG (100 μ g/mL) *in vitro* for 48 h, and then the nonadherent cells were collected and stained for CD80, MHC class I or MHC class II molecules. As shown in Fig. 1A, SCG increased the expression of CD80, MHC class I and MHC class II molecules on the cell membrane of BMDCs. SCG increased the expression of CD80 in a dose-dependent manner, with the maximal effect at a concentration of 50 μ g/mL (Fig. 1B). The enhancement of CD80 expression by SCG occurred at as low as 1 μ g/mL. These results showed that SCG induced the maturation of BMDCs *in vitro*.

LPS has been reported to be an inducer of DC activation and maturation. Next, we compared the cytokine

concentrations in the supernatants of BMDCs treated with SCG to those with LPS. BMDCs from DBA/2 mice were cultured with SCG (100 μ g/mL) or LPS (10 ng/mL) *in vitro* for 48 h, and then the supernatants were collected. The concentrations of IFN- γ , IL-12p70, IL-10, IL-6, and TNF- α were measured. As shown in Fig. 2, IL-12p70, IL-6, and TNF- α were induced by SCG. IL-10 was not induced by either stimulant. IL-6 and TNF- α were induced by SCG in a dose-dependent manner, with the maximal effect at a concentration of 100 μ g/mL (Fig. 3). The cytokine induction of SCG occurred at as low as 1 μ g/mL. These results showed that SCG induced cytokine production along with the maturation of BMDCs.

Strain difference of cytokine induction by SCG in BMDCs

We previously observed that splenocytes derived from naive DBA/2 mice strongly responded to SCG and produced higher amounts of cytokines *in vitro* than splenocytes from other strains of mice (Harada and others 2002b). To determine whether BMDCs from DBA/2 mice are also particularly sensitive to SCG, we compared the level of cytokine induction by SCG in BMDCs from various strains of mice. BMDCs from DBA/2, C57BL/6, BALB/c, C3H/HeN, and C3H/HeJ mice were cultured with SCG (100 μ g/mL) or LPS (10 ng/mL) *in vitro* for 48 h, and then the supernatants were collected. The concentrations of IL-6 and TNF- α were measured. As shown in Fig. 4, IL-6 and TNF- α were significantly induced by SCG in BMDCs from DBA/2, C57BL/6, BALB/c, C3H/HeN, and C3H/HeJ mice, and the induction of IL-6 and TNF- α by LPS was detected in BMDCs from these mice except for C3H/HeJ mice. A significantly higher level of TNF- α was induced by SCG than by LPS in DBA/2 mice (LPS, 2583 pg/mL; SCG, 9595 pg/mL). In addition, the magnitude of TNF- α and IL-6 induction in DBA/2 mice was higher than that in other strains of mice. Especially, the magnitude of TNF- α production induced by SCG in DBA/2 mice (9595 pg/mL) was at least four times higher than that in the other strains of mice (C57BL/6, 2093 pg/mL; BALB/c, 336 pg/mL; C3H/HeN, 805 pg/mL; C3H/HeJ, 900 pg/mL). These results indicate that the induction of cytokine production *in vitro* by BMDCs as well as splenocytes from DBA/2 mice is highly sensitive to SCG.

Strain difference of dectin-1 expression on BMDCs

Next, we investigated the involvement of β -glucan receptor dectin-1 in the induction of BMDC maturation by SCG. Previously, we reported that SCG-induced cytokine production from wild-type DCs was abolished in cells homozygous for dectin-1-knockout *in vitro* (Saijo and others 2007). A recent report suggested that dectin-1 can directly activate NF- κ B in DCs via the signaling adaptor molecule CARD9 (Gross and others 2006). These findings suggested that the high sensitivity to SCG in BMDCs from DBA/2 mice would be related to the level of dectin-1 expression. We compared the level of dectin-1 expression on BMDCs from DBA/2 mice to that from various strains of mice. The BMDCs from DBA/2, C57BL/6, BALB/c, C3H/HeN, and C3H/HeJ mice were

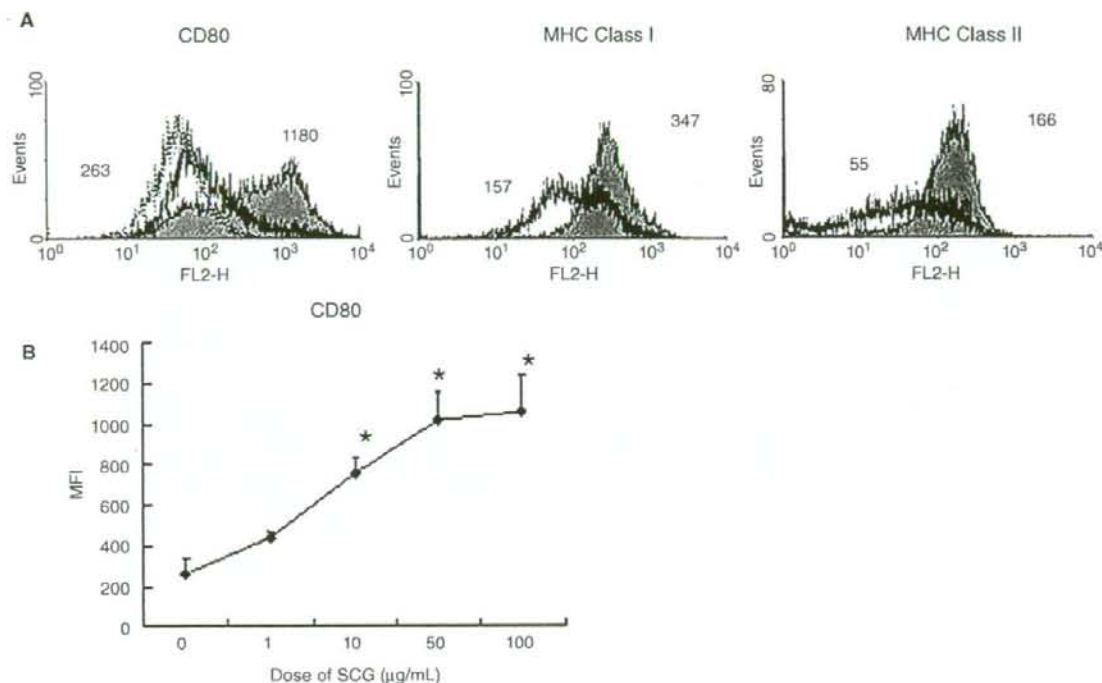


FIG. 1. Expression of surface antigens on BMDCs stimulated with SCG in DBA/2 mice. (A) BMDCs from DBA/2 mice were stimulated with SCG (100 $\mu\text{g/mL}$) and cultured for 48 h. After incubation, nonadherent cells were stained for CD11c and CD80, MHC class I or MHC class II molecules, and then analyzed using flow cytometry. The data show the expression of CD80, MHC class I and MHC class II molecules on CD11c-positive cells (thin line, isotype control; thick line, without stimulation; solid line, SCG stimulation). The values shown in the flow cytometry profiles are the mean fluorescence intensity (MFI) indexes. Data are representative of three independent experiments. (B) BMDCs from DBA/2 mice were stimulated with SCG (0, 1, 10, 50, or 100 $\mu\text{g/mL}$) and cultured for 48 h. After incubation, nonadherent cells were stained for CD11c and CD80, and then analyzed using flow cytometry. The data show the mean MFI indexes in three mice. Similar results were obtained in one other independent experiment. Significant difference from the control, * $p < 0.05$.

stained with antimouse dectin-1 (2A11). Figure 5 shows the results for the expression of dectin-1 on BMDCs. The level of dectin-1 expression on BMDCs in DBA/2 mice was significantly higher than that in the other mice. These results suggest that the high expression of dectin-1 was related to cytokine induction by SCG in BMDCs from DBA/2 mice.

Willment and others (2003) reported that dectin-1 expression was highly upregulated by GM-CSF, and that IL-10, LPS, and dexamethasone downregulated the expression of this receptor. We tested whether treatment with SCG affected the expression of dectin-1 on the surface of BMDCs. BMDCs from DBA/2 mice were stimulated with SCG (100 $\mu\text{g/mL}$) and cultured for 48 h, then stained with antimouse dectin-1 (2A11). Figure 6 shows the results for the expression of dectin-1 on the surface. The level of dectin-1 expression on BMDCs was decreased by treatment with SCG. These results suggested that treatment with SCG downregulated dectin-1 expression or internalized dectin-1 on the surface of BMDCs. Previously, we prepared two antimurine dectin-1 mAbs, 4B2

and SC30. Binding of SPG-biotin to dectin-1-transduced cells was inhibited by the 4B2 but not SC30, although SC30 had a slight competitive effect on the binding of SPG to splenocytes (Ikeda and others 2007). To confirm the effect of SCG on the expression of dectin-1, we then used 2A11, 4B2, and SC30 as detection antibodies to dectin-1. Dectin-1 on BMDCs was detected by these antibodies. The level of dectin-1 expression on SCG-treated BMDCs which detected by these antibodies were decreased (data not shown). There were no differences in the expression of dectin-1 on SCG-treated BMDCs among detected antibodies. These results indicated that treatment with SCG downregulated dectin-1 expression or internalized dectin-1 on the surface of BMDCs.

Effect of dectin-1 on cytokine induction by SCG in BMDCs

The above results suggested that the level of dectin-1 expression was related to the high sensitivity to SCG in the

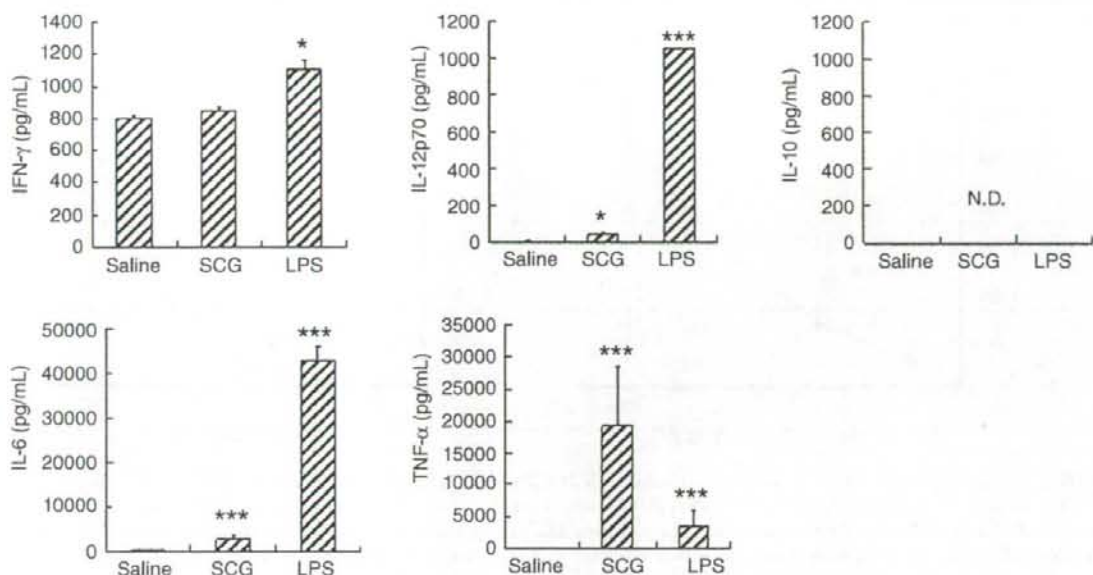


FIG. 2. Cytokine induction by SCG in BMDCs from DBA/2 mice. BMDCs from DBA/2 mice were cultured with SCG (100 μ g/ml) or LPS (10 ng/ml) *in vitro* for 48 h. After incubation, the supernatant was collected, and the concentrations of IFN- γ , IL-12p70, IL-10, IL-6, and TNF- α in the supernatant were determined using ELISA. The data represent the mean of four samples, and were reproducible in three independent experiments. Significant difference from the control, * p < 0.05, *** p < 0.001.

BMDCs from DBA/2 mice. To confirm the involvement of dectin-1 in the interaction of BMDCs with SCG, neutralization experiments were performed. Cell surface dectin-1 was blocked by neutralizing concentrations of its respective antibody (2A11, 1 μ g/ml) before BMDCs from DBA/2 or C57BL/6 mice were treated with SCG. In Fig. 7, we show that the addition of an anti-dectin-1 mAb to BMDCs blocked SCG-induced TNF- α production. These results suggest that dectin-1 is required for cytokine induction by SCG in BMDCs.

Taken together, these results suggest that the BMDCs from DBA/2 mice are highly sensitive to the cytokine-inducing activity of SCG *in vitro*, and that this high sensitivity in DBA/2 mice is related to the expression level of dectin-1.

Discussion

Antitumor immunity is coordinated by both innate and adaptive immunity, and mainly mediated by cytotoxic T cells (CTLs), natural killer (NK) cells, and natural killer T (NKT) cells. The main players within this context are DCs, which induce, coordinate, and regulate the system (Banchereau and others 2000). DCs are highly potent APCs with the unique ability of taking up and processing antigens in the peripheral blood and tissues. They subsequently migrate to the draining lymph nodes, where they present antigens to naive T lymphocytes, and thus induce a cellular immune response involving both CD4⁺ T helper 1 (Th1) cells and

cytotoxic CD8⁺ T cells. Moreover, DCs are also important in inducing humoral immunity as a result of their capacity to activate naive and memory B cells. Thus, DCs can modulate the whole immune repertoire, and therefore represent an excellent tool for immunization against cancer as well as pathogens. In the absence of stimulation, DCs remain in an immature state. Stimulation of immature DCs induces the maturation process and migration of large quantities of DCs to the draining lymph nodes to present tumor antigens to T cells. This process is associated with various coordinated events, such as the upregulation of costimulatory molecules (CD80 and CD86), loss of phagocytic receptors, and changes and upregulation of MHC class II compartments. The cell surface expression of MHC and costimulatory molecules is critical for the activation of naive T cells (Banchereau and Steinman 1998). In this study, we showed that SCG increased the expression of CD80, MHC class I and MHC class II molecules on the cell membrane of BMDCs, and induced BMDCs to produce IL-12p70, IL-6, and TNF- α , but not IL-10 (Fig. 1–3). We previously showed that SCG enhanced the expression of CD40 and CD80 on BMDCs from C57BL/6 mice (Saijo and others 2007). We also reported that β -glucan derived from *Candida albicans* increased the expression of CD86 as well as CD80, MHC class I and MHC class II molecules on BMDCs (Kikuchi and others 2002). The ability of BMDCs to uptake dextran was higher than that of BMDCs stimulated with LPS and with β -glucan. There were no differences in the uptake of dextran among LPS and β -glucan. These results indicated

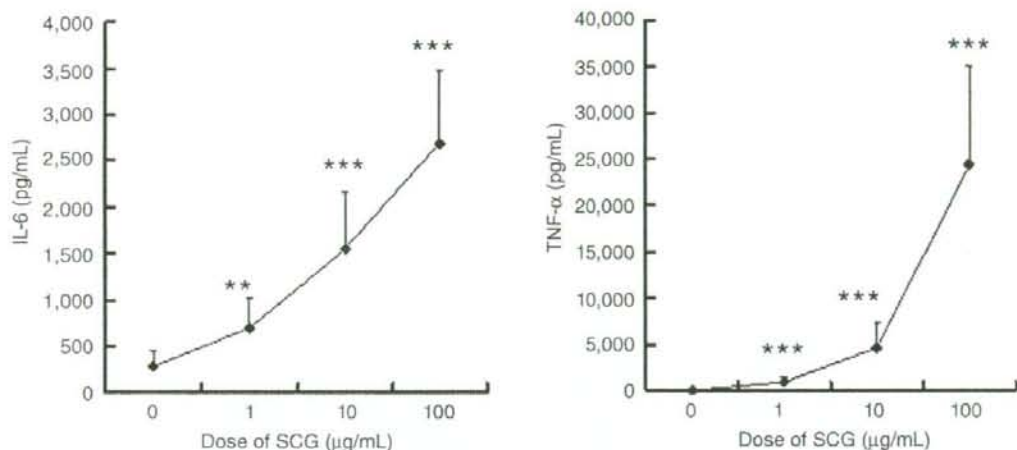


FIG. 3. Dose response of SCG for cytokine induction in BMDCs from DBA/2 mice. BMDCs from DBA/2 mice were cultured with SCG (0, 1, 10, or 100 µg/mL) *in vitro* for 48 h. After incubation, the supernatant was collected, and the concentrations of IL-6 and TNF-α in the supernatant were determined using ELISA. The data represent the mean of four samples, and were reproducible in three independent experiments. Significant difference from the control, ** $p < 0.01$, *** $p < 0.001$.

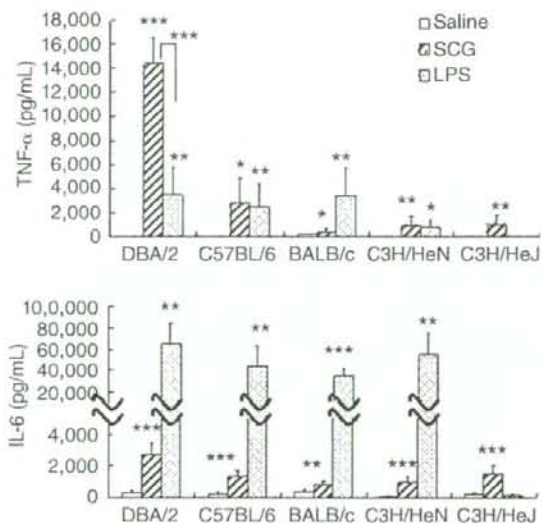


FIG. 4. Cytokine induction by SCG in BMDCs from various strains of mice. BMDCs from DBA/2, C57BL/6, BALB/c, C3H/HeN, and C3H/HeJ mice were cultured with SCG (100 µg/mL) or LPS (10 ng/mL) *in vitro* for 48 h. After incubation, the supernatant was collected, and the concentrations of IL-6 and TNF-α in the supernatant were determined using ELISA. The data represent the mean of four samples and were reproducible in three independent experiments. Significant difference from the control, * $p < 0.05$, ** $p < 0.01$, *** $p < 0.001$.

that phagocytosis by BMDCs stimulated with β-glucan decreased when maturation was augmented. These findings suggested that β-glucan was a good inducer of DC maturation in mice. The maximal effect of SCG on increase of CD80 expression were 50 µg/mL (Fig. 1B), and that on cytokine induction of SCG were 100 µg/mL (Fig. 3). On the other hand, these effects occurred at as low as 1 µg/mL. Previously, we showed that the significant amount of β-glucan, remained in liver and spleen 1 month after *i.p.* administration of β-glucan in mice (Suda and others 1992). A majority of β-glucans distributed in spleen and liver were recovered from the noncellular fraction and not from splenic macrophage and Kupffer cell fractions. These results suggested that β-glucans would not be easily incorporated by the host cells to degrade and exclude from the body. We consider that SCG at lower dose would be effective on the expression of biological activities *in vivo*. In this study, we used SCG at high dose (100 µg/mL) *in vitro* to show the difference clearly.

Early detection of potential pathogens is critical for protection against infection. Pattern-recognition receptors (PRRs), such as TLR and C-type lectins, play an important role in this process, sensing the presence of conserved molecular signatures of microbes, and signaling for leukocyte activation and induction of antimicrobial immunity. The archetypal examples of PRRs are the TLRs, which regulate proinflammatory gene expression via a conserved signaling pathway involving activation of NF-κB, mitogen-activated protein kinases (MAPKs), and interferon regulatory factors (IRFs) (Akira and Takeda 2004). Classical C-type lectins contain so-called CRDs that bind carbohydrate structures in a calcium (Ca^{2+})-dependent manner. Ca^{2+} ions are directly involved in ligand binding as well as in maintaining the structural integrity of the CRD, which is necessary for the lectin

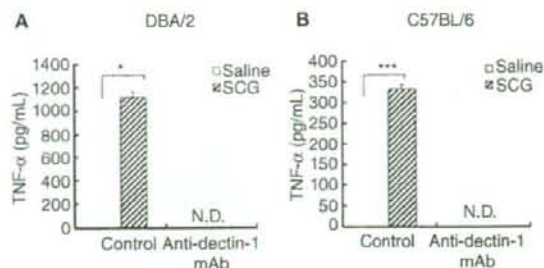


FIG. 7. Cytokine induction by SCG in BMDCs DBA/2 and C57BL/6 mice in the presence of anti-dectin-1 mAb. (A) BMDCs from DBA/2 mice were preincubated with anti-dectin-1 mAb (1 ng/mL) for 1 h. BMDCs were then challenged with SCG (1 μ g/mL) for 48 h. (B) BMDCs from C57BL/6 mice were preincubated with anti-dectin-1 mAb (1 ng/mL) for 1 h. BMDCs were then challenged with SCG (10 μ g/mL) for 48 h. After incubation, the supernatant was collected, and the TNF- α concentration in the supernatant was determined using ELISA. The data represent the mean of four samples and were reproducible in three independent experiments. Significant difference from the control, * p < 0.05, *** p < 0.001.

DBA/2 mice recognized SCG and therefore upregulated cytokines better than those from the other strains of mice (Fig. 4), which can be explained by their higher surface expression of dectin-1. TNF- α induction by SCG was inhibited by blocking of dectin-1 on BMDCs in both DBA/2 mice and C57BL/6 mice (Fig. 7). We reported that the induction of TNF, IL-12, and IFN- γ production by SCG was completely abolished in dectin-1 knockout BMDCs (Saijo and others 2007). These results indicate that dectin-1 is an important molecule in cytokine induction by SCG in BMDCs. These results also suggest that the expression level of dectin-1, as well as GM-CSF, could regulate the reactivity to β -glucan. BMDCs from C57BL/6 produced more cytokines than that from BALB/c mice (Fig. 4). On the other hand, the level of dectin-1 expression on BMDCs from BALB/c mice was higher than that from C57BL/6 mice. These results suggested that the differences in dectin-1 expression on BMDCs from the various strains did not seem to correlate with the sensitivity of BMDCs to SCG. Murine dectin-1 mRNA is alternatively spliced and generates two isoforms, a full-length dectin-1A that contains a C-type lectin-like domain, a short stalk region, a transmembrane region, and a cytoplasmic immunoreceptor tyrosine-based activation-like motif, and a stalkless dectin-1B isoform. Heinsbroek and others (2006) reported that the two isoforms exhibited differences in their ability to recognize zymosan and to induce cellular responses, such as TNF- α production, upon zymosan recognition. Although both isoforms are able to induce TNF- α production upon zymosan recognition, dectin-1B-expressing cells produce significantly more TNF- α . This finding suggests that TNF- α induction is influenced by dectin-1 structure. Macrophages from BALB/c mice expressed both

isoforms in similar amounts, whereas that from C57BL/6 mice mainly expressed the dectin-1B (Heinsbroek and others 2006). Although we did not approach the expression of each isoform on BMDCs in this study, the differences in the regulation of isoform usage would influence the cytokine induction of SCG as well as the level of dectin-1 expression.

Dectin-1 signals through a "hemITAM" motif, an immunoreceptor tyrosine-based activation motif-like sequence containing a single "YxxL" motif, that becomes phosphorylated by Src family kinases after receptor engagement. This allows recruitment of the spleen tyrosine kinase Syk, which then activates "downstream" signaling components, including the transcription factor NF- κ B (Rogers and others 2005). Activation of NF- κ B by dectin-1 requires the CARD11-related adaptor protein CARD9, which binds the adaptors MALT1 and Bcl-10 and promotes activation of the IKK kinase complex (Gross and others 2006). Leibundgut and others (2007) recently reported that dectin-1-Syk-CARD9 signaling promoted DC maturation and induced the secretion of proinflammatory cytokines, including IL-23, but little IL-12, and that DCs activated by dectin-1 engagement strongly biased Th cell differentiation to a Th-17 fate. Human DC-SIGN, which is one of the C-type lectins we described above, engagement by *Mycobacterium tuberculosis* alters TLR-induced cytokine responses (Geijtenbeek and van Kooyk 2003). Some studies demonstrated that dectin-1 collaborates with TLRs, followed by activation of transcription factor NF- κ B via MyD88, in the induction of proinflammatory cytokines. However, it remains unclear to what extent dectin-1, DC-SIGN, and other C-type lectins signal directly or simply act as TLR coreceptors. Many of the published studies regarding β -glucan-mediated signal transduction were performed using a commercially available β -glucan preparation, such as zymosan, a polysaccharide particle from the cell wall of *Saccharomyces cerevisiae*. However, we have already shown that this zymosan is very crude and commonly contains other components, including mannans, other glucans, and chitins (Ikeda and others 2005). We reported that cytokine induction by zymosan was significantly reduced by the lack of MyD88, but SCG-induced cytokine production was not affected at all (Saijo and others 2007). These facts indicate that cytokine induction via dectin-1 signaling is independent of MyD88. These findings also suggest that the high reactivity to SCG of BMDCs from DBA/2 mice is related to high expression of dectin-1, not of other TLRs.

As mentioned above, DBA/1 and DBA/2 mice are highly sensitive to SCG *in vivo* and *in vitro*. In this study, we showed that the level of dectin-1 expression of leukocytes affected the sensitivity to soluble β -glucan *in vitro*. Previously, we demonstrated that the hematopoietic response to SCG in cyclophosphamide-induced leukopenic mice was related to the enhancement of dectin-1 expression on leukocytes by treatment with cyclophosphamide (Harada and others 2006a). These results suggest that the level of dectin-1 expression could influence the bioactivities of β -glucan *in vivo* as well as *in vitro*. DBA strains are inbred strains widely used for immunological research. Collagen-induced arthritis is a well-characterized model for human rheumatoid arthritis and was developed in DBA/1 mice (Zanelli and others 1995). We have recently found that fungal β -glucan shows adjuvant

activity for the CIA model, and this activity is superior to that of Freund's complete adjuvant, because its use permits the maintenance of good physiological conditions in the mice (Hida and others 2005). Arteritis induced by *C. albicans* water-soluble fraction (CAWS), which is composed of a mannoprotein- β -glucan complex, has been shown in various strains of mice and is most serious in DBA/2 mice (Miura and others 2004). These facts suggest that DBA strains are sensitive to PAMPs, especially from fungi, such as β -glucan and mannoprotein. In the present study, we clarified in part the molecular mechanism of the induction of DC maturation by β -glucan in DBA/2 mice, and showed that it is dependent on the expression level of dectin-1. This mechanism might be related at least in part to the pathogenesis of CIA and arteritis. Many research projects are focusing on the relevant genes themselves, but the relevant environmental factors, such as chemicals and foodstuffs, are also important. Treatment with cyclophosphamide enhanced the expression of dectin-1, and the leukocytes from cyclophosphamide-treated mice acquired sensitivity to SCG-induced production of high level of cytokines (Harada and others 2006a). These results indicate that the sensitivity to β -glucan is dependent not only on relevant genes but also on external factors.

Acknowledgment

We thank Ayako Yamamoto and Junko Kita for excellent technical assistance.

References

Adachi Y, Ishii T, Ikeda Y, Hoshino A, Tamura H, Aketagawa J, Tanaka S, Ohno N. 2004. Characterization of beta-glucan recognition site on C-type lectin, dectin 1. *Infect Immun* 72:4159-4171.

Akira S, Takeda K. 2004. Toll-like receptor signalling. *Nat Rev Immunol* 4:499-511.

Banchereau J, Steinman RM. 1998. Dendritic cells and the control of immunity. *Nature* 392:245-252.

Banchereau J, Briere F, Caux C, Davoust J, Lebecque S, Liu YJ, Pulendran B, Palucka K. 2000. Immunobiology of dendritic cells. *Ann Rev Immunol* 18:767-811.

Dennehy KM, Brown GD. 2007. The role of the [beta]-glucan receptor Dectin-1 in control of fungal infection. *J Leukoc Biol* 2[Epub ahead of print].

Drickamer K. 1999. C-type lectin-like domains. *Curr Opin Struct Biol* 9:585-590.

Figdor CG, van Kooyk Y, Adema GJ. 2002. C-type lectin receptors on dendritic cells and Langerhans cells. *Nat Rev Immunol* 2:77-84.

Gantner BN, Simmons RM, Underhill DM. 2005. Dectin-1 mediates macrophage recognition of *Candida albicans* yeast but not filaments. *EMBO J* 24:1277-1286.

Geijtenbeek TB, van Kooyk Y. 2003. Pathogens target DC-SIGN to influence their fate DC-SIGN functions as a pathogen receptor with broad specificity. *APMIS* 111:698-714.

Gross O, Gewies A, Finger K, Schafer M, Sparwasser T, Peschel C, Forster I, Ruland J. 2006. Card9 controls a non-TLR signalling pathway for innate anti-fungal immunity. *Nature* 442:651-656.

Harada T, Miura NN, Adachi Y, Nakajima M, Yadamae T, Ohno N. 2002a. Effect of SCG, 1,3- β -D-glucan from *Sparassis crispa* on the hematopoietic response in cyclophosphamide induced leukopenic mice. *Biol Pharm Bull* 25:931-939.

Harada T, Miura NN, Adachi Y, Nakajima M, Yadamae T, Ohno N. 2002b. IFN- γ induction by SCG, 1,3- β -D-glucan from

Sparassis crispa, in DBA/2 mice *in vitro*. *J Interferon Cytokine Res* 22:1227-1239.

Harada T, Miura NN, Adachi Y, Nakajima M, Yadamae T, Ohno N. 2003. Antibody to soluble 1,3/1,6- β -D-glucan, SCG in sera of naive DBA/2 mice. *Biol Pharm Bull* 26:1225-1228.

Harada T, Miura NN, Adachi Y, Nakajima M, Yadamae T, Ohno N. 2004. Granulocyte-macrophage colony-stimulating factor (GM-CSF) regulates cytokine induction by 1,3- β -D-glucan SCG in DBA/2 mice *in vitro*. *J Interferon Cytokine Res* 24:478-489.

Harada T, Masuda S, Arai M, Adachi Y, Nakajima M, Yadamae T, Ohno N. 2005. Soy isoflavone aglycone modulates a hematopoietic response in combination with soluble beta-glucan: SCG. *Biol Pharm Bull* 28:2342-2345.

Harada T, Kawaminami H, Miura NN, Adachi Y, Nakajima M, Yadamae T, Ohno N. 2006a. Mechanism of enhanced hematopoietic response by soluble beta-glucan SCG in cyclophosphamide-treated mice. *Microbiol Immunol* 50:687-700.

Harada T, Kawaminami H, Miura NN, Adachi Y, Nakajima M, Yadamae T, Ohno N. 2006b. Comparison of the immunomodulating activities of 1,3- β -glucan fractions from culinary-medicinal mushroom, *Sparassis crispa* Wulf:Fr. (Aphyllphoromycetidae). *Int J Medicinal Mushrooms* 8:231-244.

Harada T, Kawaminami H, Miura NN, Adachi Y, Nakajima M, Yadamae T, Ohno N. 2006c. Cell to cell contact through ICAM-1-LFA-1 and TNF- α synergistically contributes to GM-CSF and subsequent cytokine synthesis in DBA/2 mice induced by 1,3- β -D-Glucan SCG. *J Interferon Cytokine Res* 26:235-247.

Heinsbroek SF, Taylor PR, Rosas M, Willment JA, Williams DJ, Gordon S, Brown GD. 2006. Expression of functionally different dectin-1 isoforms by murine macrophages. *J Immunol* 176:5513-5518.

Herre J, Gordon S, Brown GD. 2004. Dectin-1 and its role in the recognition of beta-glucans by macrophages. *Mol Immunol* 40:869-876.

Hida S, Miura NN, Adachi Y, Ohno N. 2005. Effect of *Candida albicans* cell wall glucan as adjuvant for induction of autoimmune arthritis in mice. *J Autoimmun* 25:93-101.

Hong F, Hansen RD, Yan J, Allendorf DJ, Baran JT, Ostroff GR, Ross GD. 2003. Beta-glucan functions as an adjuvant for monoclonal antibody immunotherapy by recruiting tumoricidal granulocytes as killer cells. *Cancer Res* 63:9023-9031.

Ikeda Y, Adachi Y, Ishibashi K, Miura N, Ohno N. 2005. Activation of toll-like receptor-mediated NF- κ B by zymosan-derived water-soluble fraction: possible contribution of endotoxin-like substances. *Immunopharmacol Immunotoxicol* 27:285-298.

Ikeda Y, Adachi Y, Ishii T, Tamura H, Aketagawa J, Tanaka S, Ohno N. 2007. Blocking effect of anti-Dectin-1 antibodies on the anti-tumor activity of 1,3- β -glucan and the binding of Dectin-1 to 1,3- β -glucan. *Biol Pharm Bull* 30:1384-1389.

Kikuchi T, Ohno N, Ohno T. 2002. Maturation of dendritic cells induced by *Candida* beta-D-glucan. *Int Immunopharmacol* 2:1503-1508.

Leibundgut-Landmann S, Gross O, Robinson MJ, Osorio F, Slack EC, Tsou SV, Schweighoffer E, Tybulewicz V, Brown GD, Ruland J, Reis E, Sousa C. 2007. Syk- and CARD9-dependent coupling of innate immunity to the induction of T helper cells that produce interleukin 17. *Nat Immunol* 8:630-638.

Miura NN, Shingo Y, Adachi Y, Okawara IA, Oharaseki T, Takahashi K, Naoe S, Suzuki K, Ohno N. 2004. Induction of coronary arteritis with administration of CAWS (*Candida albicans* water-soluble fraction) depending on mouse strains. *Immunopharmacol Immunotoxicol* 26:527-543.

Nameda S, Harada T, Miura NN, Adachi Y, Yadamae T, Nakajima M, Ohno N. 2003. Enhanced cytokine synthesis of leukocytes by a β -glucan preparation, SCG, extracted from a medicinal mushroom, *Sparassis crispa*. *Immunopharm Immunot* 25:321-335.

- Ohno N, Miura NN, Nakajima M, Yadomae T. 2000. Antitumor 1,3-beta-glucan from cultured fruit body of *Sparassis crispa*. *Biol Pharm Bull* 23:866-872.
- Ohno N, Harada T, Masuzawa S, Miura NN, Adachi Y, Nakajima M, Yadomae T. 2002. Antitumor activity and hematopoietic response of β -glucan extracted from an edible and medicinal mushroom *Sparassis crispa* wulf:Fr (Aphyllphoromycetidae). *Int J Medicinal Mushrooms* 4:13-26.
- Ohno N, Nameda S, Harada T, Miura NN, Adachi Y, Nakajima M, Yoshida K, Yoshida H, Yadomae T. 2003. Immunomodulating activity of a β -glucan preparation, SCG, extracted from a culinary-medicinal mushroom, *Sparassis crispa* Wulf:Fr. (Aphyllphoromycetidae), and application to cancer patients. *Int J Medicinal Mushrooms* 5:373-381.
- Rogers NC, Slack FC, Edwards AD, Nolte MA, Schulz O, Schweighoffer E, Williams DL, Gordon S, Tybulewicz VL, Brown GD, Reis e Sousa C. 2005. Syk-dependent cytokine induction by Dectin-1 reveals a novel pattern recognition pathway for C type lectins. *Immunity* 22:507-517.
- Saijo S, Fujikado N, Furuta T, Chung SH, Kotaki H, Seki K, Sudo K, Akira S, Adachi Y, Ohno N, Kinjo T, Nakamura K, Kawakami K, Iwakura Y. 2007. Dectin-1 is required for host defense against *Pneumocystis carinii* but not against *Candida albicans*. *Nat Immunol* 8:39-46.
- Sato T, Iwabuchi K, Nagaoka I, Adachi Y, Ohno N, Tamura H, Seyama K, Fukuchi Y, Nakayama H, Yoshizaki F, Takamori K, Ogawa H. 2006. Induction of human neutrophil chemotaxis by *Candida albicans*-derived beta-1,6-long glycoside side-chain-branched beta-glucan. *J Leukoc Biol* 80:204-211.
- Steele C, Rapaka RR, Metz A, Pop SM, Williams DL, Gordon S, Kolls JK, Brown GD. 2005. The beta-glucan receptor dectin-1 recognizes specific morphologies of *Aspergillus fumigatus*. *PLoS Pathog* 1:e42.
- Suda M, Ohno N, Adachi Y, Yadomae T. 1992. Tissue distribution of intraperitoneally administered (1 \rightarrow 3)-beta-D-glucan (SSG), a highly branched antitumor glucan, in mice. *J Pharmacobiodyn* 15:417-426.
- Sun K, Wang L, Zhang Y. 2006. Dendritic cell as therapeutic vaccines against tumors and its role in therapy for hepatocellular carcinoma. *Cell Mol Immunol* 3:197-203.
- Tada R, Harada T, Miura NN, Adachi Y, Nakajima M, Yadomae T, Ohno N. 2007. NMR characterization of the structure of a beta-(1 \rightarrow 3)-D-glucan isolate from cultured fruit bodies of *Sparassis crispa*. *Carbohydr Res* 342:2611-2618.
- Taylor PR, Tsoni SV, Willment JA, Dennehy KM, Rosas M, Findon H, Haynes K, Steele C, Botto M, Gordon S, Brown GD. 2007. Dectin-1 is required for beta-glucan recognition and control of fungal infection. *Nat Immunol* 8:31-38.
- Thoma-Uszynski S, Stenger S, Takeuchi O, Ochoa MT, Engele M, Sieling PA, Barnes PF, Rollinghoff M, Bolcskei PL, Wagner M, Akira S, Norgard MV, Belisle JT, Godowski PJ, Bloom BR, Modlin RL. 2001. Induction of direct antimicrobial activity through mammalian toll-like receptors. *Science* 291:1544-1547.
- Willment JA, Lin HH, Reid DM, Taylor PR, Williams DL, Wong SY, Gordon S, Brown GD. 2003. Dectin-1 expression and function are enhanced on alternatively activated and GM-CSF-treated macrophages and are negatively regulated by IL-10, dexamethasone, and lipopolysaccharide. *J Immunol* 171:4569-4573.
- Yadomae T. 2000. Structure and biological activities of fungal beta-1,3-glucans. *Yakugaku Zasshi* 120:413-431.
- Yadomae T, Ohno N. 1996. Structure-activity relationship of immunomodulating (1 \rightarrow 3)-beta-D-glucans. *Recent Res Devel Chem Pharm Sci* 1:23-33.
- Zanelli E, Gonzalez-Gay MA, David CS. 1995. Could HLA-DRB1 be the protective locus in rheumatoid arthritis? *Immunol Today* 16:274-278.
- Zhou T, Chen Y, Hao I, Zhang Y. 2006. DC-SIGN and immunoregulation. *Cell Mol Immunol* 3:279-283.

Address reprint requests or correspondence to:

Professor Naohito Ohno
 Laboratory for Immunopharmacology of Microbial Products
 School of Pharmacy
 Tokyo University of Pharmacy and Life Science
 1432-1 Horinouchi, Hachioji
 Tokyo 192-0392, Japan

Tel and Fax: +81-426-76-5561
 E-mail: ohnonao@ps.toyaku.ac.jp

Received XX 2008/Accepted XX 2008

AQ1: Please provide the in-text citation for this reference
 EQ1: Please provide manuscript history details.

RNA-Containing Cytoplasmic Inclusion Bodies in Ciliated Bronchial Epithelium Months to Years after Acute Kawasaki Disease

Anne H. Rowley^{1,2*}, Susan C. Baker⁴, Stanford T. Shulman¹, Francesca L. Garcia¹, Linda M. Fox⁵, Ian M. Kos¹, Susan E. Crawford³, Pierre A. Russo⁶, Rashid Hammadeh⁵, Kei Takahashi⁸, Jan M. Orenstein⁷

1 Department of Pediatrics, Northwestern University Feinberg School of Medicine, The Center for Kawasaki Disease, The Children's Memorial Hospital, Chicago, Illinois, United States of America, **2** Department of Microbiology-Immunology, Northwestern University Feinberg School of Medicine, Chicago, Illinois, United States of America, **3** Department of Pathology, Northwestern University Feinberg School of Medicine, Chicago, Illinois, United States of America, **4** Department of Microbiology and Immunology, Loyola University Stritch School of Medicine, Maywood, Illinois, United States of America, **5** Department of Pathology, Loyola University Stritch School of Medicine, Maywood, Illinois, United States of America, **6** Department of Pathology, Children's Hospital of Philadelphia, Philadelphia, Pennsylvania, United States of America, **7** Department of Pathology, George Washington University School of Medicine, Washington, D. C., United States of America, **8** Department of Pathology, Toho University School of Medicine, Tokyo, Japan

Abstract

Background: Kawasaki Disease (KD) is the most common cause of acquired heart disease in children in developed nations. The KD etiologic agent is unknown but likely to be a ubiquitous microbe that usually causes asymptomatic childhood infection, resulting in KD only in genetically susceptible individuals. KD synthetic antibodies made from prevalent IgA gene sequences in KD arterial tissue detect intracytoplasmic inclusion bodies (ICI) resembling viral ICI in acute KD but not control infant ciliated bronchial epithelium. The prevalence of ICI in late-stage KD fatalities and in older individuals with non-KD illness should be low, unless persistent infection is common.

Methods and Principal Findings: Lung tissue from late-stage KD fatalities and non-infant controls was examined by light microscopy for the presence of ICI. Nucleic acid stains and transmission electron microscopy (TEM) were performed on tissues that were strongly positive for ICI. ICI were present in ciliated bronchial epithelium in 6/7 (86%) late-stage KD fatalities and 7/27 (26%) controls ages 9–84 years ($p = 0.01$). Nucleic acid stains revealed RNA but not DNA within the ICI. ICI were also identified in lung macrophages in some KD cases. TEM of bronchial epithelium and macrophages from KD cases revealed finely granular homogeneous ICI.

Significance: These findings are consistent with a previously unidentified, ubiquitous RNA virus that forms ICI and can result in persistent infection in bronchial epithelium and macrophages as the etiologic agent of KD.

Citation: Rowley AH, Baker SC, Shulman ST, Garcia FL, Fox LM, et al (2008) RNA-Containing Cytoplasmic Inclusion Bodies in Ciliated Bronchial Epithelium Months to Years after Acute Kawasaki Disease. PLoS ONE 3(2): e1582. doi:10.1371/journal.pone.0001582

Editor: Adam Ratner, Columbia University, United States of America

Received: November 30, 2007; **Accepted:** January 15, 2008; **Published:** February 13, 2008

Copyright: © 2008 Rowley et al. This is an open-access article distributed under the terms of the Creative Commons Attribution License, which permits unrestricted use, distribution, and reproduction in any medium, provided the original author and source are credited.

Funding: Supported by NIH HL63771 (to AHR), the Kawasaki Disease Fund of Children's Memorial Hospital, and the Research Funding Committee of Loyola University Stritch School of Medicine, LU#109703 (to SCB). Sponsors/funders did not have any role in the design and conduct of the study, data collection analysis, and interpretation, or in preparation, review or approval of the manuscript.

Competing Interests: The authors have declared that no competing interests exist.

*E-mail: a-rowley@northwestern.edu

Introduction

Kawasaki Disease (KD), the most common cause of acquired heart disease in children in developed nations, is an acute systemic inflammatory illness of young children, affecting the medium-sized arteries, particularly the coronary arteries. KD is manifested by the sudden onset of high-spiking fever, rash, enanthem, exanthem, swelling and redness of the hands and feet, and cervical adenopathy in previously healthy infants and children [1]. Although these findings resolve over 1–2 weeks, 25% of untreated patients develop coronary artery abnormalities; in severe cases, myocardial infarction and sudden death can occur. Although the etiology is unknown, clinical and epidemiologic features are consistent with an ubiquitous infectious agent that usually results

in asymptomatic infection but can lead to KD in a very small subset of genetically predisposed individuals [2].

We discovered that oligoclonal IgA plasma cells infiltrate inflamed tissues in acute KD [3–5], and made synthetic versions of these oligoclonal antibodies. The KD synthetic antibodies detect antigen in ciliated bronchial epithelium of children who died of KD during the acute illness and in a subset of macrophages in acute stage inflamed KD tissues, including the coronary arteries [6,7]. We demonstrated that synthetic antibodies derived from immunoglobulin alpha sequences that are more prevalent in acute KD arterial tissue bind more strongly to the antigen in KD ciliated bronchial epithelium than do antibodies derived from immunoglobulin alpha sequences that are less prevalent in acute KD arterial tissue, a characteristic feature of an antigen-driven

antibody response [8]. Antigen was not detected in bronchial epithelium of any of 10 control infants [6,7]. Infant tissues were used as controls in these studies because they would be less likely to harbor a ubiquitous persistent or latent microbe than tissues from older children and adults, in the event that the KD agent is such a microbe. We examined acute KD ciliated bronchial epithelium using light and electron microscopy and showed that the antigen resides in intracytoplasmic inclusion bodies (ICI) that are consistent with aggregates of viral protein and nucleic acid [7].

We hypothesized that KD antigen detected in inclusion bodies during acute KD would be cleared by the immune system within the first two months after the onset of illness, when inflammation is most commonly observed in KD tissues [9]; we previously detected ICI in ciliated bronchial epithelium of 16/19 (84%) of acute KD patients but in 0/11 control infants [6,7] ($p < 0.001$). However, we recognized that ICI could be present in a small subset of older individuals with non-KD illness and of late-stage KD fatalities, because such individuals could be incidentally acutely infected or re-infected, respectively, with the KD ubiquitous respiratory microbe. If KD results from infection with a persistent or latent agent, the prevalence of ICI in KD tissues could be quite high, similar to that detected during acute infection. To determine the prevalence of ICI in these groups, we examined lung tissues from older children and adults with non-KD illness and tissues from KD patients who died ≥ 10 weeks after the onset of acute KD by light and electron microscopy.

Results

We previously reported that intracytoplasmic inclusions (ICI) in acute KD ciliated bronchial epithelium were consistent with aggregates of viral proteins and associated nucleic acids [7]. To determine whether the ICI are manifestations of an acute infection that is cleared when acute signs of inflammation are resolved in

KD (typically 8 weeks or less after the onset of fever [1]), we examined lung tissues from late-stage KD fatalities and controls. We also performed nucleic acid stains on ICI, to determine whether RNA or DNA was present.

Immunohistochemistry (IHC)

ICI were present in ciliated bronchial epithelium in 6/7 (86%) late-stage KD fatalities and 7/27 (26%) controls ages 9–84 years ($p = 0.01$). Dark brown-staining ICI, mostly supranuclear, were observed in ciliated bronchial epithelial cells from KD patients 1 (Figure 1B), 2, and 3 (Figure 2A, 2E, 2F) using synthetic antibody J; control antibody I gave negative results (Figure 2B) (Table 1). ICI were particularly numerous in KD patient 3; virtually all ciliated bronchioles had ICI. In KD patient 1, ICI were present in ciliated bronchioles in almost all blocks from different areas of the lung, but some bronchioles had many more ICI than others. In KD patient 2, ICI were less prevalent, with some bronchioles negative and others positive. In KD patients 4–6, ICI were less prevalent, with bronchi in some lung blocks entirely negative and in other lung blocks positive. ICI were not observed in available lung sections from KD patient 7, although ICI were observed in macrophages in peribronchial lymph node tissue in this patient.

In KD patients 1–6, as in the KD patients reported in our prior study [6,7] there was a striking restriction in the distribution of ICI in bronchi. ICI were not present in large bronchi completely surrounded by cartilage, but were predominately localized to the ciliated cells of the terminal or tertiary bronchi and especially the proximal bronchioles, where cartilage is absent and relatively few goblet cells are present. ICI extended to ciliated terminal bronchioles lacking goblet cells, but were not present in more distal bronchioles that lacked cilia. A subset of lung macrophages, usually peribronchial, in patients 1, 2, and 3 were positive. ICI were observed in

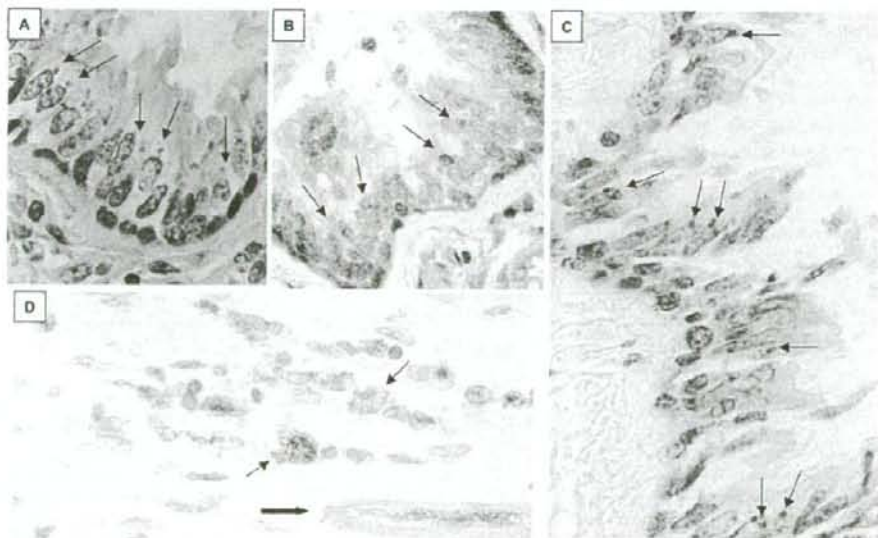


Figure 1. Light microscopic studies of tissues from KD patient 1. A, H&E of ciliated bronchial epithelium, demonstrating amphiphilic supranuclear ICI (arrows); B, IHC using synthetic antibody J of ciliated bronchial epithelium, showing ICI (arrows); C, methyl green pyronin stain of ciliated bronchial epithelium, demonstrating red ICI (arrows) indicating the presence of RNA; D, IHC using synthetic antibody J on myocardium lesion, demonstrating antigen-positive macrophages (thin arrows) infiltrating an area that has undergone myocardial dropout near a vessel (thick arrow shows single viable cardiac myocyte in this field). A–D = 40X. doi:10.1371/journal.pone.0001582.g001

macrophages in peribronchial lymph nodes in patients 2, 5 and 7; in patient 2 they appeared globular (Figure 3A). Occasionally, an antigen-positive macrophage could be observed in the lumen of a positive bronchus (Figure 2F), although most luminal macrophages were antigen-negative. Myocardium was available for study from patients 1 and 2; antigen-positive macrophages infiltrating areas of myocardial dropout near blood vessels were observed in the myocardium of patient 1 (Figure 1D). Antigen-positive macrophages were also present in the adventitia of some small coronary arteries within the myocardium. ICI were observed in ciliated bronchial epithelial cells in 7 of 27 controls ages 9–84 (Table 2). ICI in control lung were localized predominately to proximal bronchioles, as in the KD patients. Intracellular inclusion bodies were never observed in KD patients or controls.

Hematoxylin-eosin (H&E)

The lung from KD patient 1 showed evidence of acute heart failure in the form of fresh RBCs in alveolar spaces. There was also focal atelectasis and fibrin thrombi in scattered capillaries,

indicative of diffuse intravascular coagulopathy (DIC). Changes consistent with adult respiratory distress syndrome (ARDS) referred to by pathologists as diffuse alveolar damage (DAD) were observed in the lung from KD patient 2, along with pulmonary emboli without infarcts, and mild chronic bronchitis. Lung from KD patient 3 showed evidence of chronic heart failure in the form of abundant hemosiderin-laden macrophages in alveolar spaces. There was also focal atelectasis and organizing pulmonary emboli, but no infarcts. ICI were easily visualized in H&E-stained sections as supranuclear amphiphilic bodies in bronchioles from KD patient 1 (Figure 1A) and 3 (Figure 2C). Most bronchioles containing ICI were otherwise normal in appearance (Figures 1A–C, Figures 2A–F). However, shedding epithelial cells was a characteristic feature of occasional bronchioles. Lung from KD patient 4 showed bronchiolitis with atelectasis and edema, and from KD patient 5 showed ARDS and atelectasis. Lung from KD patient 6 appeared normal, and from KD patient 7 revealed changes consistent with heart failure (Table 1). Findings in the lungs of controls are indicated in Table 2.

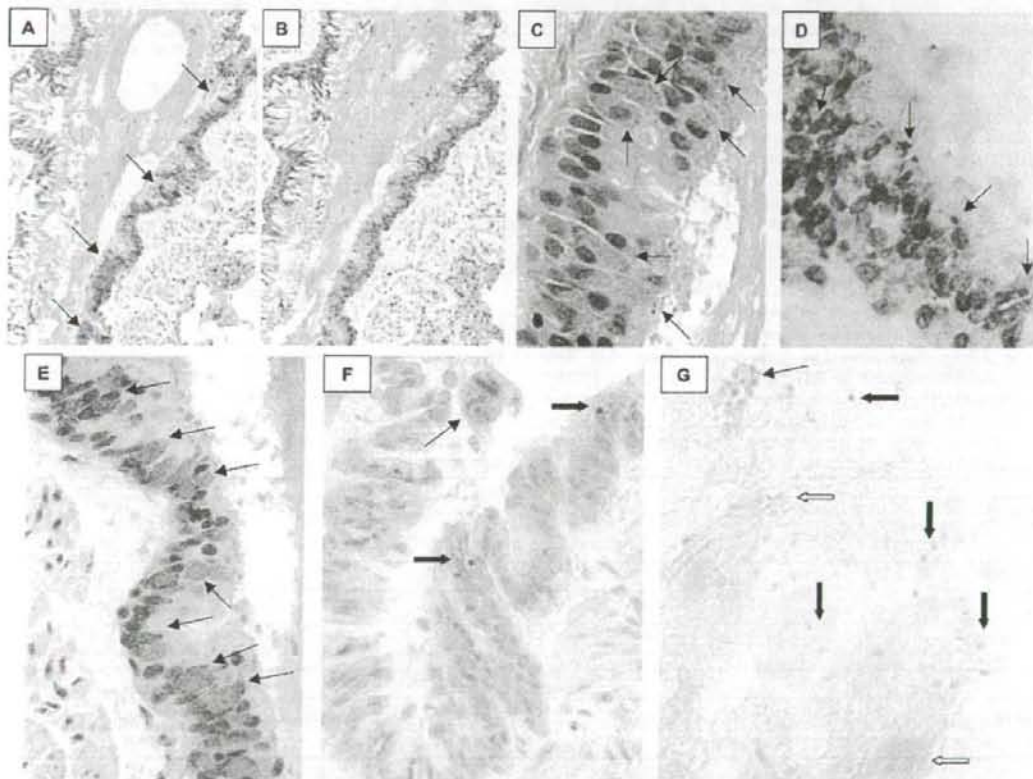


Figure 2. Light microscopic studies of ciliated bronchial epithelium from KD patient 3. A, Immunohistochemistry (IHC) using synthetic antibody J, examples of specific staining of ICI indicated with arrows; B, IHC using control antibody I, no specific staining; C, H&E stain demonstrating that ICI are visible as amphiphilic bodies (arrows); D, methyl green pyronin stain of paraffin section of a tangentially sectioned bronchus showing purple nuclei (DNA) and red ICI (RNA, arrows); E, higher-power image of Figure A, showing intense brown staining of multiple clusters of intracytoplasmic inclusion bodies (ICI, arrows); F, IHC from another bronchus, demonstrating fewer ICI (black arrows) and an IHC-positive macrophage in the lumen of the bronchus (thin arrow); G, frozen section of lung stained with methyl green pyronin; this unfixed tissue section shows typical blue-green nuclei (open arrows) and shows clusters (thin arrow) and individual (black block arrows) ICI staining red, characteristic of RNA. A,B taken with 10X objective, E=20X, C, D, F, G=40X.
doi:10.1371/journal.pone.0001582.g002

Table 1. Patients with a history of Kawasaki Disease (KD) and the pathologic findings in their lungs.

Patient	Time since KD onset	Cause of death	H&E	IHC	MGP/Feulgen	TEM
1 (F, 8 yrs, Asian)	15 months	Ventricular tachycardia	Heart failure	+	+/- (epithelium)	ICI
2 (M, 19 mos, Black)	9 months	Congestive heart failure	ARDS, PE	+	+/- (macrophage)	ICI
3 (M, 24 yrs, Hispanic)	21 years	Head trauma	Heart failure, PE	+	+/- (epithelium)	ICI
4 (NA, NA, Japanese)	14 months	Bronchiolitis	Bronchitis, atelectasis	+	ND	ND
5 (M, 5 mos, Japanese)	11 weeks	Myocardial infarction	ARDS	+	ND	ND
6 (F, 4 yrs, Japanese)	10 weeks	Status asthmaticus	No pathology	+	ND	ND
7 (F, 14 mos, Japanese)	8 months	Myocardial infarction	Heart failure	-	ND	ND

NA=not available, ND=not done, PE=pulmonary emboli, ARDS=acute respiratory distress syndrome, IHC+=indicates staining with antibody J but not antibody L; -indicates negative results with I and J
doi:10.1371/journal.pone.0001582.t001

Nucleic acid stains

The Feulgen stain, which identifies DNA, did not visualize ICI in bronchial epithelial cells in KD patients 1 or 3. However, methyl green pyronin (MGP), which stains RNA red, stained ICI red in bronchioles from both patients (Figures 1C, 2D, 2G). The cytoplasm of plasma cells in the subepithelial tissues and nucleoli also stained red and served as internal controls for RNA in the MGP preparations. In frozen sections (available only for patient 3), nuclei stained blue and ICI were red, again indicating the presence of RNA and not DNA in ICI (Figure 2G). In peribronchial lymph node of KD patient 2, MGP stains revealed red spheroids within scattered macrophages; cytoplasm of plasma cells served as an internal control for RNA and also stained red. Nucleic acid stains were not performed on tissues from patients 4–7, because fewer ICI were present.

Transmission electron microscopy (TEM)

Formalin-fixed, paraffin-embedded lung sections from KD patient 1 revealed numerous supranuclear, electron-dense, granular ICI in ciliated bronchial epithelial cells (Figure 4A). Rare alveolar macrophages in KD patient 1 were noted to have perinuclear, finely granular rounded bodies similar to those seen within the bronchial epithelium (Figure 4B), and occasional macrophages in peribronchial lymph nodes from KD patient 2 contained large finely granular ICI (Figure 3B).

Frozen lung from KD patient 3 placed into glutaraldehyde allowed for improved visualization of intracellular structures compared with tissue previously embedded in paraffin from the same patient. Rough endoplasmic reticulum, mitochondria, lysosomes and nuclei were all well visualized in glutaraldehyde-fixed ciliated bronchial epithelial cells (Figure 5A). Numerous ICI of varying electron-density, likely corresponding to the concentration of the protein and nucleic acid contents, were observed predominantly in a supranuclear location in KD patient 3 (Figure 5A); higher-power views indicated that ICI were mostly granular and smooth surfaced and did not appear to be membrane-bound (Figure 5B). However, fine detail was lost during freezing; for example, it was not possible to determine whether or not ICI represented aggregates of nucleocapsids. No viral particles or other microbial elements were identified in any cells, including those containing ICI.

No intranuclear inclusion bodies were observed by TEM in KD patients 1, 2, or 3.

Discussion

We previously reported that KD synthetic antibodies detect antigen in ciliated bronchial epithelium of acute KD patients (75% of these patients were infants), but not of infant controls [6,7]. The antigen was not any of 40 common inflammatory proteins [6], and

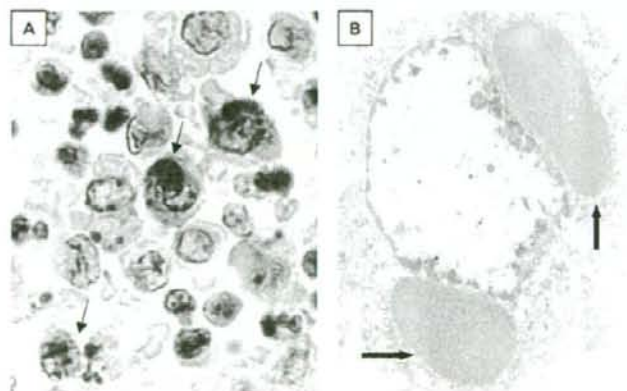


Figure 3. Peribronchial lymph node from KD patient 2. A, IHC using synthetic antibody J, showing antigen-positive macrophages containing spheroid bodies (arrows); B, transmission electron microscopy (TEM) of macrophage, showing two large, finely granular ICI (arrows). A=40X, B=20,000X.
doi:10.1371/journal.pone.0001582.g003

Table 2. Controls and the pathologic findings in their lungs.

Control	Cause of death or underlying illness	H&E	IHC
1 (83 years, F)	Cerebrovascular accident, diabetes	Heart failure	+
2 (76 years, M)	Cerebrovascular accident	COPD, pneumonia	+
3 (22 years, F)	Meningioma, renal failure, urosepsis	Heart failure, bronchitis	+
4 (18 years, F)	Renal transplant, myocardial infarction	Heart failure, bronchitis	+
5 (59 years, M)	Non-small cell carcinoma	COPD, heart failure, atelectasis	+
6 (16 years, M)	Heart transplant, coronary vasculopathy	COPD, heart failure	+
7 (71 years, F)	Squamous cell carcinoma	Heart failure, atelectasis	+
8 (81 years, F)	Cerebrovascular accident	COPD	-
9 (61 years, M)	Adenocarcinoma	Heart failure	-
10 (69 years, F)	Squamous cell carcinoma	Heart failure	-
11 (52 years, F)	Emphysema	COPD, heart failure	-
12 (66 years, M)	Adenocarcinoma	Normal	-
13 (37 years, F)	Adenocarcinoma	Heart failure	-
14 (NA, M)	Adenocarcinoma	Heart failure	-
15 (63 years, M)	Poorly differentiated adenocarcinoma	Heart failure, hemorrhage	-
16 (48 years, M)	Emphysema	Heart failure	-
17 (73 years, M)	Myocardial infarction	Normal	-
18 (63 years, M)	Cardiac arrest, diabetes	Edema	-
19 (79 years, M)	Myocardial infarction, Parkinson's disease	COPD, heart failure	-
20 (84 years, F)	Peripheral vascular disease	COPD, heart failure	-
21 (76 years, M)	Cardiac failure	COPD, heart failure	-
22 (66 years, M)	Intracranial hemorrhage, kidney transplant	Heart failure, pneumonitis	-
23 (14 years, F)	Truncus arteriosus, GI bleed	Pneumonia, edema, heart failure	-
24 (17 years, F)	SLE, multiorgan dysfunction, shock	Heart failure	-
25 (9 years, M)	Medulloblastoma, stem cell transplant	Septic emboli, infarcts	-
26 25 (67 years, M)	Squamous cell carcinoma	Edema, hemorrhage, heart failure	-
27 (79 years, M)	Adenocarcinoma	COPD, heart failure, bronchitis	-

NA = not available, COPD = chronic obstructive pulmonary disease, SLE = systemic lupus erythematosus, IHC = + indicates staining with antibody 1 but not antibody 1- indicates negative results with 1 and J
doi:10.1371/journal.pone.0001582.t002

further study indicated that the antigen was localized to ICI that appeared consistent with aggregates of viral protein and nucleic acid [7]. We initially hypothesized that ICI were present only during acute KD and were subsequently cleared by the immune system. However, in the present study, KD antigen was detected in ICI in ciliated bronchial epithelium in 6 of 7 (86%) late-stage KD fatalities and in 7 of 27 (26%) older childhood or adult controls ($p = 0.01$). The very high rate of detection of ICI in late-stage KD fatalities is strongly suggestive of establishment of persistent or latent infection following the acute illness. The detection of ICI in 86% of late-stage KD fatalities is virtually identical to the 84% rate of detection (16/19) of ICI in our two combined previous studies of KD fatalities in the first two months after the onset of illness [6,7]. It is possible that an even higher percentage of KD patients harbor ICI in ciliated bronchial epithelium, but that insufficient archival tissue was available from some patients to demonstrate the ICI. In several KD patients in whom an initially tested lung section did not reveal ICI, examination of sections from additional lung blocks clearly showed ICI. Because epidemiologic data are consistent with a ubiquitous agent as the cause of KD [1], with frequent asymptomatic or mildly symptomatic infection in the general population, establishment of a persistent infection by the agent in some individuals would likely result in the detection of ICI

in a subset of older children and adult controls, consistent with our findings. Although re-infection is a possibility, we believe that persistent infection is more likely, in view of the high rate of ICI detection in late-stage KD fatalities and because acute infection in one-quarter of a group of random controls seems unlikely even for a ubiquitous infectious agent.

It is notable that in the classic 1980 study by Amano and colleagues on the general pathology of acute KD, inflammatory lesions were unusual in most organs later than 60 days after the onset of fever, but "in the lung, spleen, salivary gland or lymph nodes, inflammation was considered to be persistent or recurrent [9]." The authors studied tissues from 9 KD children who died after the 60th day of illness, with death ranging from 66 days to 4.5 years after the onset; 7/9 had evidence of bronchitis. Antigen was not detected in either of 2 salivary gland tissues available to us from acute KD fatalities (data not shown); we have previously reported positive results of antigen detection in macrophages in lymph nodes and spleen in children with acute KD [6], and in this study we report antigen detection in the lung of KD patients months to years after the acute illness.

Several RNA viruses, most notably the human and animal paramyxoviruses, have been associated with persistence in infected cells. Persistence of cytoplasmic and nuclear inclusion bodies in

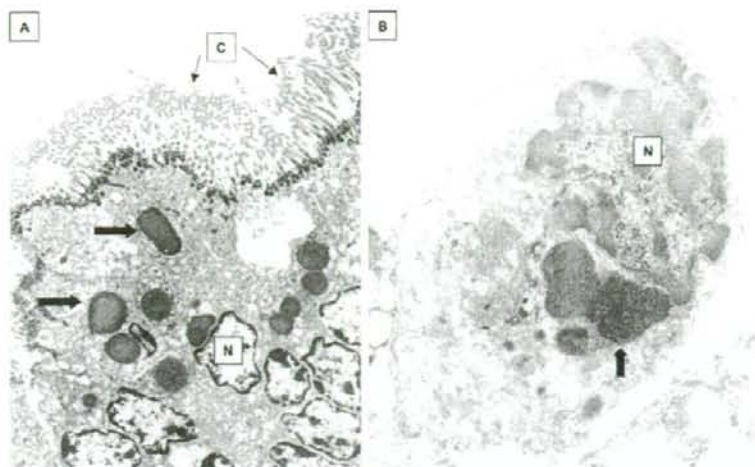


Figure 4. TEM of formalin-fixed, paraffin-embedded lung from KD patient 1. A, ciliated bronchial epithelium demonstrating electron-dense apical ICI (block arrows). B, alveolar macrophage, demonstrating perinuclear, finely granular spheroid bodies similar to those seen within the bronchial epithelium (block arrow). N = nucleus, C = cilia. A = 9,500X, B = 26,000X.
doi:10.1371/journal.pone.0001582.g004

human brain was demonstrated in subacute sclerosing panencephalitis (SSPE), a persistent measles virus infection. Canine distemper virus can result in persistence of ICI in tissue culture cells [10]. Randall and colleagues showed that simian virus 5 (SV5) can establish persistent infection by remaining inactive in ICI [11–13]. In contrast to measles virus in SSPE, infectious SV5 virus occasionally can be reactivated from ICI in persistent infection

[11]. It has been proposed by these authors that some paramyxoviruses may form ICI as a viral defense mechanism to evade the immune system [13]. In this model, when the virus is exposed to interferon, it halts production of its glycoproteins, which are no longer expressed on the surface of infected cells, and viral nucleocapsid proteins accumulate in ICI [13]. Because viral glycoproteins are not expressed on the cell surface, the immune

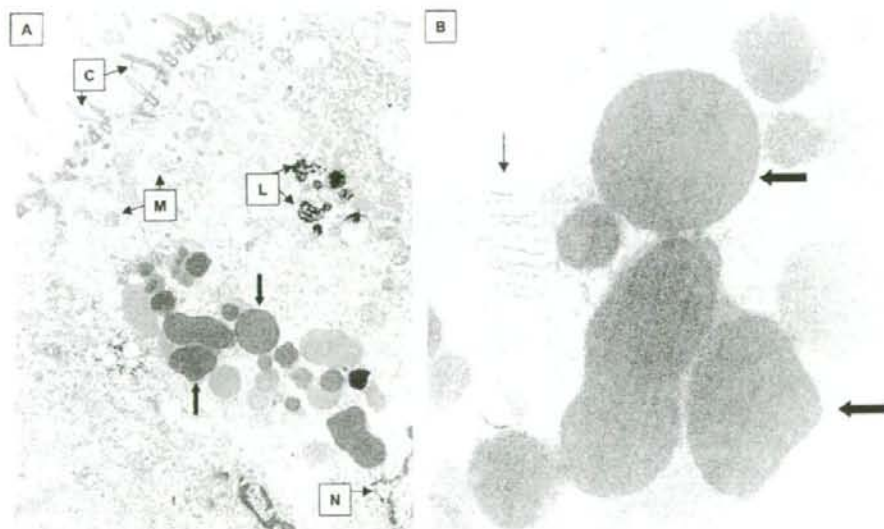


Figure 5. Transmission electron microscopy (TEM) of ciliated bronchial epithelium from glutaraldehyde-fixed, previously frozen lung from KD patient 3. A) Lower power image demonstrating finely granular, variably electron-dense ICI (block arrows). N = nucleus, L = lysosomes, M = mitochondria, C = cilia. B) Higher power image of ICI (block arrows). Note rough endoplasmic reticulum (thin arrow). ICI are spherical and do not appear membrane-bound. A = 14,000X, B = 52,000X.
doi:10.1371/journal.pone.0001582.g005

system does not recognize the cell as infected. The virus can remain inactive within ICI for prolonged periods of time but occasionally can be reactivated and viral replication reinitiated [12]. The infected host could then release virus into the environment until a secondary immune response once again forces the virus to recede back into inactive ICI.

At least 20 cases of Kawasaki Disease-like illness have been reported in HIV-infected adults [14]. In these patients, moderate to severe immune dysfunction and high viral loads have been characteristic [14]. This has led some authors to propose that these patients are experiencing reactivation of a persistent infectious agent of KD following childhood infection [15]. A persistent infectious agent could also explain recurrences of KD in at least 1–3% of affected children [1].

Bronchial epithelial cells undergo turnover when injured, and therefore, cells containing ICI could be destroyed or shed. However, our hypothesis is that newly formed ciliated bronchial epithelial cells could become infected during reactivation of the putative viral agent in adjacent cells containing ICI; the agent would have a short time period to replicate and be shed before memory immune responses would force it to recede back into inclusion bodies. The clinical illness of KD would only recur in those individuals in whom memory immune responses were not adequate to prevent systemic spread of infection. Individuals in whom ICI form and persist could intermittently shed infectious virus over a long period of time [12]; this would be a very effective way for a ubiquitous respiratory virus to spread through the population. Healthy asymptomatic individuals in isolation at the South Pole have been reported to intermittently shed parainfluenza virus over a 6–8 month period, with two outbreaks of respiratory illness occurring within that 8 month period best explained as being initiated by persistently infected individuals [16]. Lung tissue was not available from persistently infected individuals in this study, and it is not known whether these human parainfluenza viruses formed ICI in bronchial epithelium. Other viruses such as human metapneumovirus and rhinovirus have been reported to result in persistent infection in immunocompromised hosts [17,18]. Viral persistence related to the formation of ICI has not been demonstrated in these studies, and clearly the KD agent is different from the known human respiratory viruses.

Our findings emphasize the likelihood that macrophages play a key role in the pathogenesis of KD. It is not clear whether antigen-positive macrophages in KD patients are scavengers and/or whether they become infected with the KD agent. Macrophages could be responsible for uptake of the agent from bronchioles and delivery to other distal sites, such as the coronary arteries, as they circulate through the bloodstream and into tissues. To date, we have not observed antigen-positive lymphocytes or neutrophils in acute or late-stage KD patient tissues.

ICI in KD patients and controls were strikingly localized to the ciliated epithelial cells of smaller bronchi and bronchioles. ICI were not present in non-ciliated cells or in ciliated cells of trachea or large bronchi completely surrounded by cartilage. This remarkable restriction in localization of ICI leads us to speculate that only the ciliated epithelial cells lining the smaller bronchi and bronchioles express a receptor that facilitates entry of the KD agent into the cell or a cellular gene that facilitates formation of ICI in these cells.

We are utilizing various methods to identify the proteins and nucleic acids within the ICI, and we believe that this information will likely lead to the identification of the KD etiologic agent. These efforts have been hampered by the extreme scarcity of fresh tissue samples from KD fatalities. Several studies in which RNA extracted from KD tissue has been analyzed on viral microarrays

have so far not yielded a positive result (data not shown). We believe it likely that the KD agent is a currently unknown RNA virus that may not show significant homology to known viruses. Efforts to obtain fresh lung and coronary artery tissue from KD fatalities for molecular studies and for direct placement into glutaraldehyde for optimal ultrastructural experiments should continue. In addition, our data indicate that antigen-positive unfixed tissue from adult controls could potentially be utilized in these experiments.

In conclusion, we report that ICI are present in ciliated bronchial epithelial cells in about 85% of KD patients who died months to years after the acute illness, that the antigen detected by KD synthetic antibody and identified within ICI in ciliated bronchial epithelial cells could also be identified in a subset of macrophages in lung, peribronchial lymph nodes, and damaged myocardium from some KD patients months to years after acute KD, that the nucleic acid within these ICI is RNA and not DNA, and that ICI can be observed in ciliated bronchial epithelium in about 25% of controls ages 9–84. These findings provide new directions in the search for the etiologic agent of KD, and point to a ubiquitous, previously unrecognized RNA virus that can result in persistent infection as the causative agent.

Materials and Methods

Patients and Specimens

Formalin-fixed, paraffin-embedded lung tissue was available for light microscopy from all of 7 late-stage KD fatalities (in whom death occurred ≥ 10 weeks after the onset of fever) and 27 controls. Three KD patients died of myocardial infarction or congestive heart failure as a result of coronary artery aneurysms, one died postoperatively following a procedure to resect giant aneurysms, and three died of causes unrelated to KD (Table 1). Selected other tissues were available for study from KD patients 1 and 2, such as myocardium and lymph node.

Patient 1 developed KD at age 7 years. She was initially treated with antibiotics, and KD was diagnosed when echocardiography showed a large coronary artery aneurysm. She was treated with two infusions of IVIG and maintained on long-term coumadin and aspirin. Fifteen months after the onset of illness, she underwent elective resection of bilateral giant coronary artery aneurysms with homograft placement, but died two hours postoperatively following the development of hypotension and ventricular tachycardia. The ethnicity of patient 1 was described as "Asian", but further information was not available.

Patient 2 was admitted at 19 months of age with cough and congestion for one week without fever; rales were detected on examination of the chest. The clinical diagnosis was possible myocarditis or endocarditis. Despite intensive care, he suffered multiple cardiac arrests and died 3 days after admission. Autopsy revealed severe congestive heart failure, dilated coronary arteries, necrotizing arteritis of all the coronary arteries with occlusions, and areas of myocardial infarction. In retrospect, the child had had a febrile illness at 10 months of age that was diagnosed as a streptococcal infection, but likely represented an episode of KD.

Frozen lung tissue from KD patient 3 was provided by the National Disease Research Interchange (NDRI). Patient 3, a 24-year-old male, had KD at age 3. Because of confidentiality issues, it was not possible to obtain further history regarding the KD illness. The patient had Wolf-Parkinson-White syndrome and underwent an ablation procedure 7 years prior to death. The patient was found underneath a car with severe head trauma, and toxicology studies were positive for cocaine and phencyclidine (PCP). He was reported to be well prior to this event. His heart grossly appeared normal, and was used for transplant. One lung

was used for transplant, and frozen tissue from the other lung was available for research. Serologic studies for HIV, syphilis, hepatitis B and hepatitis C infection were negative. Information regarding the condition of the recipient(s) of the other lung and heart was not available to NDRI because of confidentiality issues.

Patients 4 died of acute bronchitis and patient 6 died of asthma. Patients 5 and 7 died of myocardial infarction as a late consequence of KD (Table 1).

Control tissues were obtained from grossly normal-appearing areas of lung at the time of lung transplantation, lung biopsy, or autopsy. Lung tissue from controls 1,2, 8,9,17–19, and 20–22 were provided by NDRI. For controls, information regarding a past history of KD, a prolonged febrile illness during childhood, and/or the degree of immunosuppression administered to the cancer and transplant patients was not available.

Frozen lung tissue from KD patient 3 (Table 1) was partially thawed, bronchi were dissected, and the tissue was placed in glutaraldehyde for examination by TEM. Formalin-fixed, paraffin-embedded lung sections and blocks from KD patient 1 (Table 1) were studied by TEM. The present study was approved by the Institutional Review Boards of Children's Memorial Hospital and Loyola University Medical Center.

Synthetic KD antibodies

Synthetic KD antibodies were made as previously described [6]. IHC was performed with synthetic antibodies J and I [7]. Antibody J shows strong binding to acute KD but not to control infant ciliated bronchial epithelium; control antibody I does not demonstrate binding [6,7,8].

Immunohistochemistry

Formalin-fixed, paraffin-embedded tissue sections were deparaffinized by use of xylene, rehydrated, and heated in 10 mM sodium citrate buffer (pH 6.0), to enhance antigen retrieval [6]. Sections were incubated with 10–15 micrograms/ml biotinylated synthetic antibody J or I and color developed using the Vectastain Elite ABC kit (Vector). Diaminobenzidine tetrahydrochloride was used as a reaction product, to generate a brown stain. Sections

were lightly counterstained with hematoxylin. We recorded positive results when strong brown staining of ICI was observed in ciliated bronchial epithelial cells, or in tissue macrophages.

Hematoxylin-eosin, methyl green pyronin (MGP), and Feulgen stains

Nucleic acid stains were performed on tissues from KD patients 1 and 3, which were strongly positive for ICI. Standard hematoxylin-eosin, MGP, and Feulgen staining was performed on formalin-fixed, paraffin-embedded lung tissues. MGP staining was also performed on frozen sections of lung from KD patient 3, and formalin-fixed peribronchial lymph node from KD patient 2.

Transmission electron microscopy (TEM)

TEM was performed on tissues from KD patients 1 and 3, because ICI were especially abundant in these patients. TEM was performed in 2 different laboratories. At Loyola University, resin blocks were made from formalin-fixed, paraffin-embedded tissue sections from KD patients 1 and 3 after IHC with synthetic antibody, to allow for accurate localization of ICI within bronchi, as previously described [7]. At George Washington University, pieces of formalin-fixed, paraffin-embedded tissues were excised directly from areas of tissue blocks that were positive by IHC, as previously described [7]. In addition, TEM was performed on frozen lung from KD patient 3 that was placed into glutaraldehyde, as described above.

Statistical analysis

The prevalence of ICI in KD patients and controls was compared using a two-tailed Fisher's exact test, with a $p \leq 0.05$ considered significant.

Author Contributions

Conceived and designed the experiments: JO SB AR SS LF SC. Performed the experiments: JO AR FG LF IK RH. Analyzed the data: JO SB AR SS FG LF IK SC PR RH KT. Contributed reagents/materials/analysis tools: AR PR RH KT. Wrote the paper: JO SB AR SS FG LF IK SC PR KT.

References

- Rowley AH, Shulman ST (2007) Kawasaki Disease. In: Kliegman R, Behrman R, Jenson H, Stanton B, eds. *Nelson Textbook of Pediatrics* 18th edition. Philadelphia: Elsevier. pp 1036–42.
- Rowley AH, Shulman ST (2007) New developments in the search for the etiologic agent of Kawasaki disease. *Current Opinion in Pediatrics* 19: 71–74.
- Rowley AH, Ezekiel CA, Jack HM, Shulman ST, Baker SC (1997) IgA plasma cells in vascular tissue of patients with Kawasaki syndrome. *J Immunol* 159: 5946–55.
- Rowley AH, Shulman ST, Mask CA, Finn LS, Terai M, et al. (2000) IgA plasma cell infiltration of proximal respiratory tract, pancreas, kidney, and coronary artery in acute Kawasaki disease. *J Infect Dis* 182: 1183–91.
- Rowley AH, Shulman ST, Spike BT, Mask CA, Baker SC (2001) Oligoclonal IgA response in the vascular wall in acute Kawasaki disease. *J Immunol* 166: 1334–43.
- Rowley AH, Baker SC, Shulman ST, Garcia FL, Guzman-Cottrill JA, et al. (2004) Detection of antigen in bronchial epithelium and macrophages in acute Kawasaki disease by use of synthetic antibody. *J Infect Dis* 190: 856–65.
- Rowley AH, Baker SC, Shulman ST, Fox LM, Takahashi K, et al. (2005) Cytoplasmic inclusion bodies are detected by synthetic antibody in ciliated bronchial epithelium during acute Kawasaki disease. *J Infect Dis* 192: 1757–66.
- Rowley AH, Shulman ST, Garcia FL, Guzman-Cottrill JA, Miura M, et al. (2005) Cloning the arterial IgA antibody response during acute Kawasaki disease. *J Immunol* 175: 8386–8391.
- Amano S, Hazama F, Kubagawa H, Tasaka K, Haehara H, et al. (1980) General pathology of Kawasaki Disease. *Acta Pathol Jpn* 30: 681–694.
- Narang HK (1962) Ultrastructural study of long-term canine distemper virus infection in tissue culture cells. *Infection and Immunity* 36: 310–319.
- Chatzidimitrou N, Young D, Andrejeva J, Goodbourn S, Randall RE (2002) Differences in interferon sensitivity and biological properties of two related isolates of simian virus 5: a model for virus persistence. *Virology* 293: 234–242.
- Frazer R, Young DF, Randall RE (1994) Evidence that the paramyxovirus simian virus 5 can establish quiescent infections by remaining inactive in cytoplasmic inclusion bodies. *J General Virology* 75: 3525–3539.
- Carlos TS, Frazer R, Randall RE (2005) Interferon-induced alterations in the pattern of parainfluenza virus 5 transcription and protein synthesis and the induction of virus inclusion bodies. *J Virol* 79: 14112–14121.
- Stankovic K, Mialhes P, Bessou D, Ferry T, Brousseau C, et al. (2007) Kawasaki-like syndromes in HIV-infected adults. *Journal of Infection* 55: 488–94.
- Johnson RM, Little JR, Storch GA (2001) Kawasaki-like syndromes associated with Human Immunodeficiency Virus Infection. *Clinical Infectious Diseases* 32: 1628–34.
- Muchmore HG, Parkinson AJ, Humphries JE, Scott EN, McIntosh DA, et al. (1981) Persistent parainfluenza virus shedding during isolation at the South Pole. *Nature (London)* 289: 187–189.
- Kaiser L, Aubert JD, Paché JC, Deffrenz C, Rochat T, et al. (2006) Chronic rhinoviral infection in lung transplant recipients. *Am J Respir Crit Care Med* 174: 1392–9.
- Debiaggi M, Canducci F, Sampaolo M, Marinozzi MC, Parra M, et al. (2006) Persistent symptomless human metapneumovirus infection in hematopoietic stem cell transplant recipients. *J Infect Dis* 194: 474–478.

急性期川崎病血管炎の病理

大原 関利章 横内 幸 伊原 文恵
若山 恵 高橋 啓

東邦大学医学部病院病理学講座

要約：川崎病は、血管炎症候群に含まれる小児の急性熱性疾患である。冠状動脈が高頻度に侵襲され血栓性閉塞がもたらされるため、小児期における虚血性心疾患の原因となる。形態学的に認識可能な川崎病血管炎の最も初期の変化は、発症後6日頃からみられる中膜の水腫性疎開性変化と呼ばれる滲出性病変である。10病日頃には、内膜および外膜に炎症細胞浸潤が認められるようになり、炎症はただちに極期に達して血管壁の全層にわたる汎血管炎が生じる。そして、12病日頃には、血管破壊に基づく動脈瘤の形成がみられる。組織学的には、マクロファージ主体の増殖性肉芽腫性炎であるが、病初期には相当数の好中球が病変局所に出現しており、血管壁の傷害には活性化マクロファージや好中球によって産生された炎症性サイトカイン、ミエロペルオキシダーゼ、好中球エラスターゼ等の因子が関与していると考えられる。

東邦医学会誌 55(2):129-131, 2008

KEYWORDS : Kawasaki disease, vasculitis, coronary arteritis, coronary aneurysm, pathology

川崎病は、血管炎症候群に含まれる小児の急性熱性疾患である。本症では、冠状動脈が高頻度に侵襲され、冠状動脈炎に起因する動脈瘤の形成が川崎病血管炎の最大の特徴と言える。動脈瘤の血栓性閉塞は虚血性心疾患の原因となり、患児の予後に影響を及ぼす。急性期の炎症反応を可能な限り早期に終息させ、合併症である冠状動脈瘤の発生を抑制することが川崎病治療の最も重要な点であるが、このためには川崎病動脈炎の急性期の病理学的特徴を知ることがきわめて大切である。

本稿では、川崎病急性期の血管病変の病理学的特徴について概説する。併せて病変局所における炎症性サイトカインや好中球の関わりについて最近の分子生物学的手法に基づく知見を紹介したい。

急性期川崎病血管炎の病理学的特徴

川崎病は、「川崎病診断の手引き」に記載されている主要6症状の組み合わせによって臨床的に診断される疾患であるが、本症に特徴的な病理組織学的所見が存在する。

血管炎症候群では、疾患ごとに病変分布や侵襲される血管径に差があり、このことが各疾患の臨床的特徴を大きく

左右する。川崎病では、中型動脈が侵襲されやすく、特に実質臓器外の動脈に病変が惹起されるという特徴がある。病変発生頻度が最も高く、患児の予後に影響を及ぼすのは冠状動脈である^{1,2)}。大動脈との分岐部から心筋に入る前までの筋層外冠状動脈に病変が惹起されやすい。次に多いのは腎臓であるが、ここでも病変は腎動脈から葉間動脈レベルの実質外の動脈に分布する³⁾。肺、生殖器周囲、腸間膜等の動脈も侵襲を受けやすい。

川崎病血管炎のもう1つの病理学的な特徴は、急性炎症としての定型的経過を辿る点にある。すなわち、川崎病血管炎は滲出反応ではじまり、次いで炎症細胞浸潤が惹起され、極期を迎えたのち、徐々に炎症が消退して治癒あるいは器質化に至るといった一峰性の推移を示す。侵襲される臓器によって血管炎の組織学的時相が若干異なることはあっても、多発性動脈炎のように新旧の病変が混在することはない。川崎病で最も早期に認識できる形態学的変化は、中膜の水腫性疎開性変化と呼ばれる滲出反応である。発症後6～8日死亡例にみられ、中膜の外膜側に生じる水腫によって中膜平滑筋細胞が離解し、その配列が疎になる。10病日頃になると動脈の内膜側および外膜側の両方から炎症